Photocatalytic Hydrogen Evolution from Water Using Copper Gallium Sulfide under Visible-Light Irradiation

Masashi Tabata, Kazuhiko Maeda, Takahiro Ishihara, Tsutomu Minegishi, Tsuyoshi Takata, and Kazunari Domen*

Department of Chemical System Engineering, The University of Tokyo, 7-3-1 Hongo, Bunkyo-ku, Tokyo 113-8656, Japan

Received: April 8, 2010

Copper gallium sulfide with a chalcopyrite-type structure ($CuGa_3S_5$) and a band gap of ca. 2.4 eV was prepared by a solid-state reaction. The as-prepared $CuGa_3S_5$ exhibited photocatalytic hydrogen evolution activity in an aqueous solution containing Na_2S and Na_2SO_3 as sacrificial electron donors under visible-light irradiation ($\lambda > 420$ nm), even without a cocatalyst, such as platinum (Pt). The photocatalytic activity, however, was improved by the deposition of noble metal cocatalysts. Among the noble metals tested, rhodium (Rh) was found to be the most effective cocatalyst to improve the H_2 evolution activity, which was 2.5 times that achieved without a cocatalyst. Dispersion of base sulfides, including nickel sulfide (NiS) and iron sulfide (FeS), into the reactant solution containing $CuGa_3S_5$ also increased the activity. The activity under optimized conditions (5.0 wt % NiS/$CuGa_3S_5$) was 3 times that of a similarly optimized Rh/$CuGa_3S_5$. The results of electrochemical measurements and photocatalytic reactions suggested that NiS suspended in the reactant solution accepts electrons from the excited state of $CuGa_3S_5$ to reduce H^+ into H_2 when NiS and $CuGa_3S_5$ particles collide with each other in the reactant solution.

1. Introduction

Photocatalytic hydrogen production from water using semiconductor particles is an attractive means of converting solar energy into chemical energy.[1] Many active photocatalysts for splitting water under ultraviolet (UV) irradiation ($\lambda < 400$ nm) have been reported,[1c,d] and some have achieved high quantum yields.[2] However, for more efficient utilization of solar energy, photocatalysts that can function efficiently under visible light ($\lambda > 400$ nm) must be developed. As it is generally difficult to achieve overall water splitting under visible light due to the uphill nature of the reaction, sacrificial reagents, such as methanol or silver nitrate, which act as hole or electron scavengers, have been used to evaluate the photocatalytic activity of materials.[1b,d] The use of proper sacrificial electron donors that irreversibly scavenge photogenerated holes makes it possible to effectively promote hydrogen evolution from water. Metal sulfides have attracted attention for use as photocatalysts in sacrificial H_2 evolution from water containing sulfide and/or sulfate ions as electron donors.[3−12]

In most cases, active photocatalytic materials are composed of a semiconductor photocatalyst and a cocatalyst.[1b,d] Cocatalysts, usually in the form of nanoparticles, are loaded onto the semiconductor surface, and play an essential role in the photocatalytic reaction by providing active sites for redox reactions. Therefore, the loading of proper cocatalysts can greatly enhance the photocatalytic activity of a given material.[13] Kudo et al. reported that ternary metal sulfides loaded with nanoparticulate noble metals (e.g., Pt and Ru) function as highly active photocatalysts for H_2 evolution from an aqueous Na_2S and Na_2SO_3 solution under visible light, with apparent quantum yields of several tens of percent at 420 nm.[5] Very recently, it was reported that cadmium sulfide (CdS) has a high activity for the photoreduction of H^+ to H_2 in an aqueous solution containing proper electron donors under visible-light irradiation, if it is carefully prepared and/or modified by the proper cocatalysts.[8−11] It has been generally believed that intimate interaction (e.g., junction-structure) between a photocatalyst and a cocatalyst is required to obtain a highly active photocatalytic material because the interfacial structure plays a critical role in the electron-transfer process. This idea is supported by previous experimental results with metal sulfides[10b] and other photocatalysts.[14,15] In addition, it is generally known that noble metals function as efficient cocatalysts for H_2 evolution because of their high exchange-current density and low activation energy, compared with base metals, such as Fe or Ni.

In this study, we discuss an exceptional case, in which copper gallium sulfide ($CuGa_3S_5$) dispersed in an aqueous Na_2S and Na_2SO_3 solution containing base metal sulfide cocatalysts for H_2 evolution exhibited a much higher activity than physically contacting noble metal/$CuGa_3S_5$. The gallium-rich copper gallium sulfide, $CuGa_3S_5$, belongs to the I−III−VI_2 family of chalcopyrite semiconductors, of which $CuGaS_2$ is the prototype member. The schematic structure of $CuGaS_2$ is shown in Figure 1.[16] In this work, we report photocatalytic H_2 evolution using $CuGa_3S_5$ under visible-light irradiation ($\lambda > 420$ nm) and a unique reaction behavior in combination with several new sulfide cocatalysts.

2. Experimental Methods

2.1. Preparation of Photocatalysts. $CuGa_3S_5$ was obtained by heating a stoichiometric mixture of Cu_2S (Koujyundo Chemical, 99%), Ga_2S_3 (Koujyundo Chemical, 99.99%), and a small amount (0.25 wt %) of S (Wako Pure Chemical Industries, Ltd., 99%) in a sealed quartz tube under vacuum at 1073 K for 24 h. CdS powder (99%) was provided by Wako Pure Chemical Industries, Ltd. and used without further purification.

* To whom correspondence should be addressed. Tel: +81-3-5841-1148. Fax: +81-3-5841-8838. E-mail: domen@chemsys.t.u-tokyo.ac.jp.

10.1021/jp103158f
Published on Web 06/04/2010

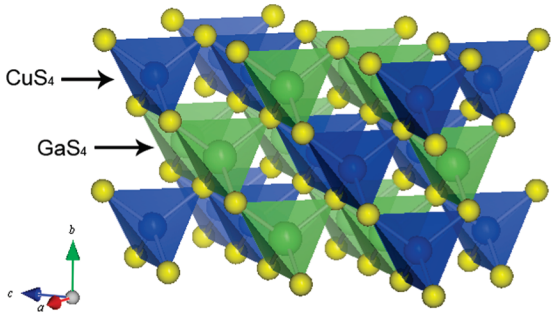

Figure 1. Crystal structure of $CuGaS_2$ (ICSD No. 28736).

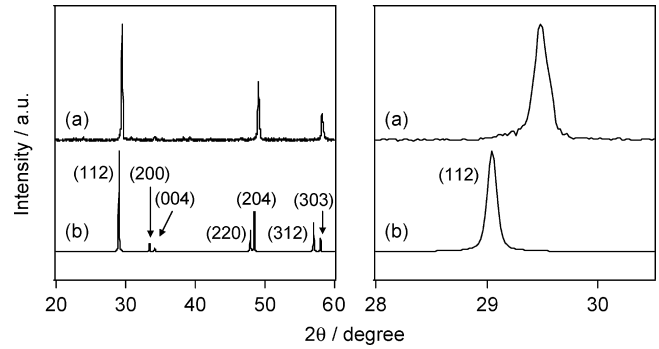

Figure 2. XRD patterns of (a) $CuGa_3S_5$ and a (b) $CuGaS_2$ reference.

$Sm_2Ti_2S_2O_5$[17] was prepared by a previously reported H_2S gas sulfurization method.[17b] Samarium titanate ($Sm_2Ti_2O_7$) was prepared by the polymerized complex method[18] using $Ti(OiPr)_4$ and $Sm(NO_3)_3 \cdot 6H_2O$ as starting materials. Ethylene glycol and methanol were employed as solvents, and anhydrous citric acid was employed as a complexing agent to immobilize Ti and Sm ions. After polymerization of a mixture containing stoichiometric amounts of Sm and Ti (Sm/Ti = 1), samarium titanates were obtained by calcination at 773 K for 12 h in air. This samarium titanate $Sm_2Ti_2O_7$ is referred to as the oxide precursor. $Sm_2Ti_2S_2O_5$ was prepared from the oxide precursor by calcination at 1173 K for 1 h under a H_2S flow (10 mL·min^{-1}), followed by heating at 473 K for 2 h in air to remove the adsorbed sulfur S^0 species from the surface of the sample.

The loading of noble metals, such as Pt, Rh, and Ir, on $CuGa_3S_5$ was performed by photodeposition. An aqueous solution containing a metal cation, $H_2PtCl_6 \cdot 6H_2O$ (Wako Pure Chemical Industries, Ltd., 98.5+%), $RhCl_3 \cdot 3H_2O$ (Wako Pure Chemical Industries, Ltd., 95.0+%), or $Na_2IrCl_6 \cdot 6H_2O$ (Kanto Chemical Co., Inc., 99.0%), was added to a suspension of photocatalyst, and then in situ photochemical deposition[19] was conducted.

Transition-metal sulfides, nickel sulfide (NiS), iron sulfide (FeS), ruthenium sulfide (Ru_2S_3), silver sulfide (Ag_2S), cobalt sulfide (CoS), palladium sulfide (PdS), and copper sulfide (CuS), were prepared in situ and employed as cocatalysts as follows. An aqueous solution containing a metal cation, $Ni(NO_3)_2 \cdot 6H_2O$ (Wako Pure Chemical Industries, Ltd., 99.9%), $FeCl_2 \cdot 4H_2O$ (Wako Pure Chemical Industries, Ltd., 99.0−102.0%), $RuCl_3 \cdot nH_2O$ (Kanto Chemical Co., Inc., 99.9%), $AgNO_3$ (Kanto Chemical Co., Inc., 99.8%), $Co(NO_3)_2 \cdot 6H_2O$ (Wako Pure Chemical Industries, Ltd., 98.0%), $Na_2PdCl_4 \cdot 3H_2O$ (Wako Pure Chemical Industries, Ltd., 95.0+%), or $Cu(NO_3)_2 \cdot 3H_2O$ (Wako Pure Chemical Industries, Ltd., 99.9%), was added dropwise to a suspension of photocatalyst powder dispersed in the reaction solution (Na_2S and Na_2SO_3 aqueous solution) just before the photocatalytic reaction. The formation of the transition-metal sulfides were confirmed by color changes of the reaction solutions.[20]

2.2. Characterization. The prepared samples were studied by powder X-ray diffraction (XRD, RINT-UltimaIII, Rigaku, Cu Kα), scanning electron microscopy (SEM, S-4700, Hitachi), and UV−visible diffuse reflectance spectroscopy (DRS, V-560, JASCO). The Brunauer−Emmett−Teller (BET) surface area was measured using a BELSORP-mini instrument (BET Japan) at liquid nitrogen temperature.

2.3. Photocatalytic Reaction. Photocatalytic reactions were carried out in a side-irradiation-type Pyrex reaction cell connected to a closed gas circulation and evacuation system. Photocatalyst powder (0.05 g) was suspended in 250 mL of an aqueous solution containing 10 mM Na_2S and 10 mM Na_2SO_3 as electron donors. The suspension was thoroughly degassed and then exposed to argon (5 kPa). The suspension was irradiated using a Xe lamp (300 W) fitted with a cold mirror (CM-1) and a cutoff filter to eliminate UV light. The evolved gases were analyzed by online gas chromatography. The quantum efficiency (Φ) was calculated using the following equation

$$\Phi(\%) = 2R/I \times 100$$

where R is the H_2 evolution rate (molecules·h^{-1}) and I is the rate of introduction of incident photons into the reaction vessel. The absorption rate of incident photons was measured using a photodiode and was typically 1.1×10^{22} photons·h^{-1} at $420 < \lambda < 520$ nm. It was assumed that the quantum efficiency was constant in the wavelength range of 420−520 nm for H_2 evolution. Therefore, the quantum efficiency obtained in this work can be regarded as an averaged apparent quantum efficiency.

2.4. Electrochemical Measurements. NiS film electrodes (1×3 cm^2) were prepared by electrophoretic deposition[21] on conducting glass supports (F-doped SnO_2). NiS powder was prepared by adding $Ni(NO_3)_2 \cdot 6H_2O$ to a Na_2S aqueous solution (S/Ni = 3 by molar ratio), followed by washing with distilled water. A platinum wire and a Ag/AgCl electrode were used as counter and reference electrodes, respectively. The potential of the working electrode was controlled by a potentiostat. Na_2SO_4 aqueous solution (0.1 M, pH = 6) was used as an electrolyte solution for electrochemical measurements. The solution was purged with argon gas before the measurements, which were conducted at room temperature.

3. Results and Discussion

3.1. Characterization of $CuGa_3S_5$. Figure 2 shows an XRD pattern from copper gallium sulfide ($CuGa_3S_5$) obtained by a solid-state reaction, along with that of a $CuGaS_2$ reference (ICSD No. 28736). The diffraction pattern of the prepared sample was similar to that of chalcopyrite $CuGaS_2$, indicating that the prepared sample crystallized in a chalcopyrite-type structure. However, each diffraction peak of the prepared copper gallium sulfide appeared at a slightly higher 2θ angle than the corresponding $CuGaS_2$ peak, indicating that the prepared sample had lattice parameters smaller than those of $CuGaS_2$. Because the ionic radius of Cu^+ (0.74 Å) is larger than that of Ga^{3+} (0.61 Å),[22] a decrease in the Cu/Ga molar ratio in copper gallium sulfides results in a diffraction peak shift. Therefore, the observed peak shift seems reasonable. It has been reported that compounds with a chalcopyrite-type structure appear to tolerate a large range of anion-to-cation off-stoichiometry and that some

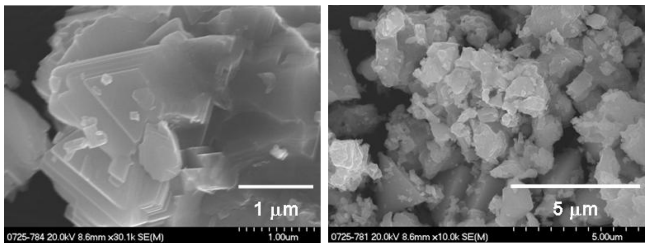

Figure 3. SEM images of $CuGa_3S_5$.

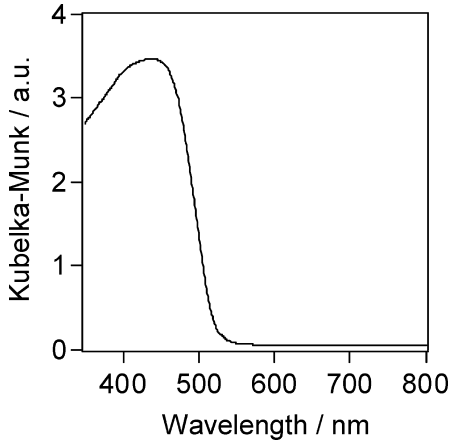

Figure 4. DRS of $CuGa_3S_5$.

copper indium selenides with several compositions, such as $CuInSe_2$, $CuIn_3Se_5$, and $CuIn_5Se_8$, could be successfully synthesized.[23] Considering these reports, it is likely that copper gallium sulfide with a Ga-rich composition (Ga/Cu = 3) is also stable and maintains a chalcopyrite-type structure.

The surface morphology of $CuGa_3S_5$ was studied by SEM. As shown in Figure 3, the particle size of $CuGa_3S_5$ was 0.1−3 μm. Some pyramidal particles were observed as aggregated secondary particles. The specific surface area, as measured by N_2 adsorption at 77 K, was 1.0 $m^2\ g^{-1}$.

Figure 4 shows a DRS of $CuGa_3S_5$. The absorption edge of $CuGa_3S_5$ was approximately 520 nm, and the band-gap energy was estimated to be 2.4 eV. Similarly, the band-gap energy of $CuGaS_2$ prepared by a solid-state reaction was estimated to be 2.3 eV. Therefore, $CuGa_3S_5$ has a slightly larger band gap than $CuGaS_2$. According to a previous report,[23a] copper indium selenides with an In-rich composition ($CuIn_3Se_5$ and $CuIn_5Se_8$) also had larger band gaps than $CuInSe_2$. The increase in the band-gap energy of $CuIn_3Se_5$ and $CuIn_5Se_8$ was mainly due to a lowering of the valence band maximum (VBM) because the In-rich composition resulted in a weaker hybridization between Cu 3d and Se 4p orbitals, which form the upper valence bands. A similar phenomenon occurred in the copper gallium sulfides. Therefore, $CuGa_3S_5$ has a larger band gap, due to its lower VBM, than $CuGaS_2$.

3.2. Photocatalytic H_2 Evolution Using $CuGa_3S_5$ with Various Cocatalysts. $CuGa_3S_5$ was active for H_2 evolution from an aqueous Na_2S and Na_2SO_3 solution under visible-light irradiation ($\lambda > 420$ nm) even without cocatalysts, producing ~15 $\mu mol \cdot h^{-1}$ of H_2. With modification by noble metal cocatalysts, however, the activity was increased, depending on the cocatalyst employed and the loading amount. Figure 5 shows the dependence of the H_2 evolution rate from an aqueous Na_2S and Na_2SO_3 solution over $CuGa_3S_5$ on the loading amount of several noble metal cocatalysts (Pt, Rh, and Ir), which were relatively effective among the noble metals examined. These noble metals are well-known cocatalysts, which promote the

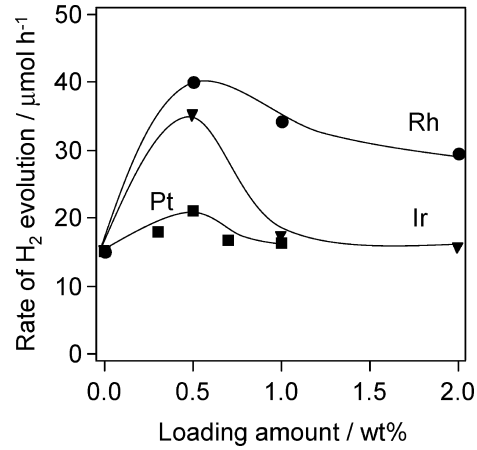

Figure 5. Rate of H_2 evolution over $CuGa_3S_5$ under visible light ($\lambda >$ 420 nm) as a function of the loading amount of noble metal (Pt, Rh, and Ir). Reaction conditions: catalyst, 0.05 g; 10 mM Na_2S and 10 mM Na_2SO_3 aqueous solution, 250 mL; light source, xenon lamp (300 W) fitted with a cold mirror (CM-1) and a cutoff filter; reaction vessel, Pyrex side-irradiation type.

reduction of H^+ to H_2.[1c] In all cases, the rate of H_2 evolution was enhanced with increasing cocatalyst loading, reaching a maximum at 0.5 wt %, beyond which the rate began to gradually decrease. Among the noble metals examined, a 0.5 wt % Rh loading provided the highest rate of H_2 evolution (40 $\mu mol \cdot h^{-1}$) using $CuGa_3S_5$. It has been reported many times that the rate of H_2 evolution from aqueous solutions containing sacrificial electron donors can be enhanced for a given metal sulfide by increasing the noble metal loading, but that excess loading results in reduced activity.[3b,8,10] The increase in H_2 evolution rate corresponds to the increased density of the loaded noble metal, which can trap excited electrons to form H_2 evolution sites. On the other hand, excessive noble metal loading leads to aggregation, hindering light absorption by $CuGa_3S_5$ and decreasing the activity.

Recently, Li et al. reported that certain metal sulfides, such as MoS_2, act as a new type of cocatalyst and promote the reduction reaction with CdS as a photocatalyst.[10,11] This sulfide is also attractive as a water reduction catalyst for chalcogenide-based p-type semiconductor electrodes in a water-splitting photoelectrochemical cell.[24] To further explore new sulfide cocatalysts that can promote water reduction, we attempted to apply transition-metal sulfides, including NiS, FeS, Ru_2S_3, Ag_2S, CoS, PdS, and CuS. Although some of these are unstable under ambient conditions, due to facile hydrolysis into the corresponding hydroxide or oxide phase, they are quite stable in an aqueous solution containing a sufficient concentration of sulfide ions. We, therefore, employed an "in-situ" preparation of sulfide cocatalysts by dispersing the corresponding precursors (nitrates or chlorides) into an aqueous Na_2S and Na_2SO_3 solution. After dispersing the precursors, precipitates with various colors, depending on the metal, were immediately produced. The production of a given sulfide was confirmed by the color of the suspension.[20] The as-prepared sulfide suspension was employed as a reactant solution containing a given sulfide cocatalyst.

Table 1 lists the H_2 evolution rates from an aqueous Na_2S and Na_2SO_3 solution containing various transition-metal sulfide cocatalysts and $CuGa_3S_5$ photocatalyst under visible light. At a 0.5 wt % cocatalyst concentration, NiS- and FeS-based systems had a distinct promotional effect on H_2 evolution over $CuGa_3S_5$, resulting in higher performance (~50 $\mu mol \cdot h^{-1}$) than the optimized case using Rh as a noble metal cocatalyst (40 $\mu mol \cdot h^{-1}$). As shown in Figure 6, the H_2 evolution activity was

TABLE 1: Rate of H_2 Evolution from $CuGa_3S_5$ Loaded with Various Cocatalysts Based on Transition-Metal Sulfides (0.5 wt %) from an Aqueous Na_2S (10 mM) and Na_2SO_3 (10 mM) Solution under Visible Light ($\lambda > 420$ nm)[a]

entry	cocatalyst	rate of H_2 evolution/μmol h^{-1}
1	none	15
2	NiS	49
3	FeS	38
4	Ru_2S_3	29
5	Ag_2S	26
6	CoS	23
7	PdS	21
8	CuS	13

[a] Reaction conditions: catalyst, 0.05 g; aqueous solution, 250 mL; light source, xenon lamp (300 W) fitted with a cutoff filter; reaction vessel, Pyrex side-irradiation type.

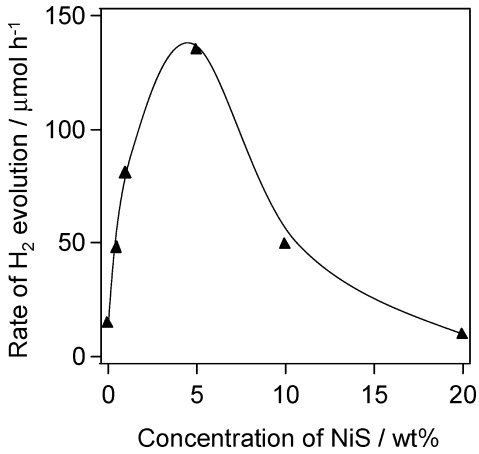

Figure 6. Rate of H_2 evolution over $CuGa_3S_5$ from an aqueous solution containing NiS under visible light ($\lambda > 420$ nm) as a function of NiS concentration. Reaction conditions: catalyst, 0.05 g; 10 mM Na_2S and 10 mM Na_2SO_3 aqueous solution, 250 mL; light source, xenon lamp (300 W) fitted with a cold mirror (CM-1) and a cutoff filter; reaction vessel, Pyrex side-irradiation type.

also dependent on the concentration of the sulfide suspension. Increasing the concentration of NiS in the reactant solution resulted in a marked enhancement of activity. However, too large an increase in the NiS concentration led to a drop in activity from the maximum value. At 5.0 wt % NiS, the highest activity was obtained, with an apparent quantum yield of ca. 1.3%. The activity of the optimized NiS/$CuGa_3S_5$ system was 6 times that of $CuGa_3S_5$ alone and triple that of the optimized Rh/$CuGa_3S_5$ system. The promotional effect of NiS on H_2 evolution by $CuGa_3S_5$ was clearly observed.

Figure 7 shows the dependence of the H_2 evolution rate from an aqueous Na_2S and Na_2SO_3 solution containing 5.0 wt % NiS and $CuGa_3S_5$ on the cutoff wavelength of the incident light. The rates of H_2 evolution decreased with increasing cutoff wavelength, and the longest wavelength available for photoreaction corresponded to the absorption edge of $CuGa_3S_5$. In addition, H_2 evolution did not proceed on NiS/$CuGa_3S_5$ in the dark, and no H_2 evolution occurred from NiS without $CuGa_3S_5$, even under visible-light irradiation. Therefore, the photocatalytic H_2 evolution was driven by the band-gap photoexcitation of $CuGa_3S_5$, and the NiS dispersed in the reactant solution functioned as a cocatalyst. Copper gallium sulfides with other compositions, such as $CuGaS_2$ and $CuGa_5S_8$, were also prepared by a solid-state reaction, and the H_2 evolution activities were investigated under the same reaction conditions. At present, however, $CuGa_3S_5$ always showed the highest activity, regardless of surface modification.

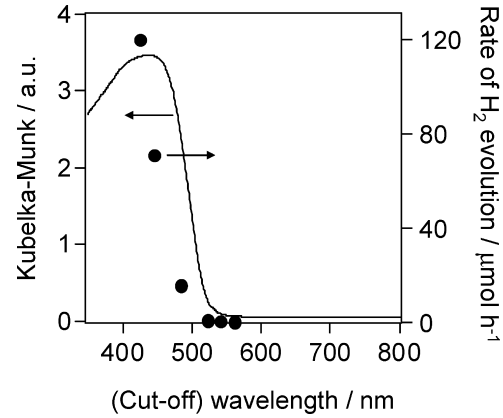

Figure 7. Rate of H_2 evolution over $CuGa_3S_5$ from an aqueous solution containing NiS (5.0 wt %) under visible light ($\lambda > 420$ nm) as a function of the cutoff wavelength of incident light. Reaction conditions: catalyst, 0.05 g; 10 mM Na_2S and 10 mM Na_2SO_3 aqueous solution, 250 mL; light source, xenon lamp (300 W) fitted with a cold mirror (CM-1) and a cutoff filter; reaction vessel, Pyrex side-irradiation type. The DRS for $CuGa_3S_5$ is also shown.

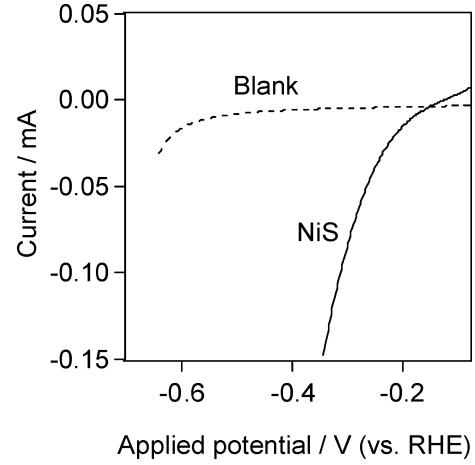

Figure 8. Current−voltage curve for a NiS electrode. Scan rate = 20 $mV \cdot s^{-1}$.

3.3. Function of NiS in H_2 Evolution Using $CuGa_3S_5$. The above results suggest that base metal sulfide particles suspended in the reactant solution assist redox reactions occurring on the $CuGa_3S_5$ surface, thereby enhancing the H_2 evolution rate. To further examine the function of NiS in H_2 evolution by $CuGa_3S_5$, electrochemical measurements were conducted using porous NiS electrodes in pure water, and the overvoltage of cathodic H_2 evolution on NiS was examined. As shown in Figure 8, a cathodic current was observed at potentials more negative than −0.2 V (vs RHE). This suggests that the NiS employed in this work functioned

TABLE 2: Rate of H_2 Evolution on Various Photocatalysts, with and without NiS (0.5 wt %) Loading, from an Aqueous Na_2S (10 mM) and Na_2SO_3 (10 mM) Solution under Visible Light ($\lambda > 420$ nm)[a]

		rate of H_2 evolution/μmol h^{-1}	
entry	cocatalyst	without NiS	with NiS
1	$CuGa_3S_5$	15	49
2	CdS	2	1
3	$Sm_2Ti_2S_2O_5$	0	19

[a] Reaction conditions: catalyst, 0.05 g; aqueous solution, 250 mL; light source, xenon lamp (300 W) fitted with a cutoff filter; reaction vessel, Pyrex side-irradiation type.

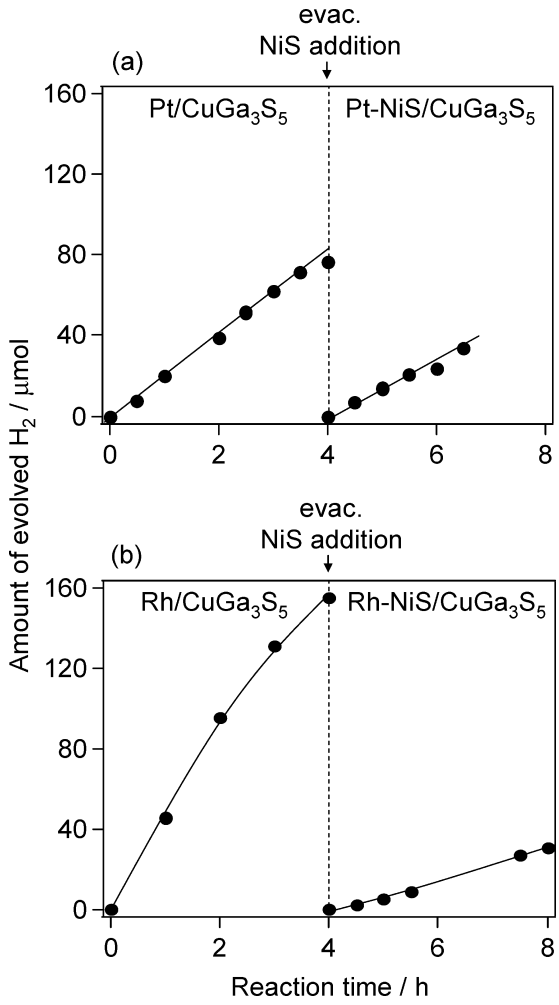

Figure 9. Time course of H_2 evolution under visible light ($\lambda > 420$ nm) over (a) Pt(0.5 wt %)/$CuGa_3S_5$ (first run) and Pt−NiS(5.0 wt %)/$CuGa_3S_5$ (second run) and (b) Rh(0.5 wt %)/$CuGa_3S_5$ (first run) and Rh−NiS(5.0 wt %)/$CuGa_3S_5$ (second run). Reaction conditions: catalyst, 0.05 g; 10 mM Na_2S and 10 mM Na_2SO_3 aqueous solution, 250 mL; light source, xenon lamp (300 W) fitted with a cold mirror (CM-1) and a cutoff filter; reaction vessel, Pyrex side-irradiation type.

as a cocatalyst, promoting the reduction of H^+ to H_2 on $CuGa_3S_5$, although the onset potential was lower than that of Pt (−0.05 V vs RHE).[9] As mentioned earlier, detailed investigation of NiS precipitates was difficult because the β-NiS employed in this work is unstable in air. In previous studies, however, it was reported that nickel sulfides act as good electrocatalysts for cathodic H_2 evolution in water electrolysis.[25] These reports also support the above-mentioned idea that NiS acts as a reduction cocatalyst.

In conventional photocatalytic systems based on particle suspensions for water splitting, a cocatalyst and a photocatalyst are combined to form a composite structure before they are used in a reaction. This is because interfacial electron transfer between the two components is critically important to maximize the overall efficiency. An interesting result obtained through the present study is that a physically mixed system, NiS/$CuGa_3S_5$, gave a higher rate of H_2 evolution than a conventional composite structure, noble metal/$CuGa_3S_5$, despite the fact that NiS is inferior to noble metals like Pt in its overpotential for H_2 evolution. This strongly suggests that interfacial electron transfer from the conduction band of $CuGa_3S_5$ to NiS is more facile than that from $CuGa_3S_5$ to noble metals, even though there is no physical junction between the $CuGa_3S_5$ and the NiS. It is most likely that interfacial electron transfer occurs when $CuGa_3S_5$ and NiS particles collide with each other. This idea is supported by the observation that the rate of H_2 evolution by $CuGa_3S_5$ was enhanced with increasing NiS concentration (Figure 6). Some photocatalytic H_2 evolution systems through a similar interparticle electron-transfer mechanism have also been reported previously.[26−28]

Using other sulfide-based photocatalysts, $Sm_2Ti_2S_2O_5$ and CdS, the effect of NiS was examined in a similar manner (see Table 2). Previous studies indicated that photodeposition of Pt onto these photocatalysts resulted in an improved activity for H_2 evolution from an aqueous Na_2S and Na_2SO_3 solution.[9,17a] The NiS cocatalyst did enhance the activity of $Sm_2Ti_2S_2O_5$; however, there was little enhancement of CdS. These results suggest that the effect of the NiS cocatalyst on H_2 evolution depends on which photocatalyst is employed. The importance of the particular combination of photocatalyst and cocatalyst in terms of electron transfer has been suggested in several other recent reports.[29,30]

To further investigate the reaction behavior, 0.5 wt % Pt- or Rh-loaded $CuGa_3S_5$ was dispersed in an aqueous Na_2S and Na_2SO_3 solution containing 5.0 wt % NiS, and the H_2 evolution rates were monitored. Interestingly, as shown in Figure 9, no promotional NiS effect was observed; the H_2 evolution activity from an aqueous Na_2S and Na_2SO_3 solution containing NiS was lower (14 and 8 μmol·h^{-1} for Pt- and Rh-loaded $CuGa_3S_5$, respectively) than that from a pure Na_2S−Na_2SO_3 solution (20 and 40 μmol·h^{-1} for Pt- and Rh-loaded $CuGa_3S_5$, respectively). The decrease in activity was presumably due to a light-filtering effect of suspended NiS particles. Li et al. reported that Pt and PdS function as effective cocatalysts in photocatalytic H_2 evolution by CdS and that the activity can be further enhanced when they are coloaded (Pt−PdS/CdS).[11] In that case, it was

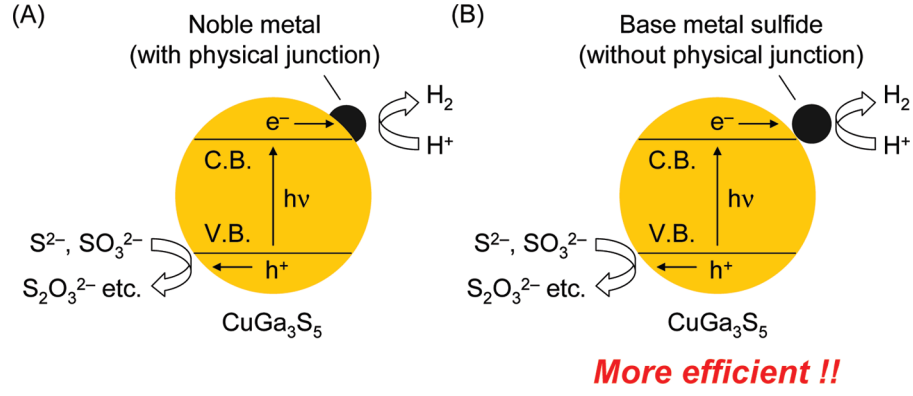

Figure 10. Schematic illustration of the proposed reaction mechanism for the photocatalytic H_2 evolution from $CuGa_3S_5$ with different types of cocatalyst: (A) noble metal and (B) base metal sulfides.

claimed that Pt acts as a cocatalyst to promote reduction by photogenerated electrons, while PdS promotes oxidation by photogenerated holes. Therefore, Pt−PdS/CdS exhibited a higher activity than Pt/CdS or PdS/CdS because the functions of Pt and PdS are different. In the present case, on the other hand, both the noble metals (Pt or Rh) and NiS cocatalyst promote reduction by photogenerated electrons, as mentioned above. Photoexcited electrons in $CuGa_3S_5$ are presumed to move instantly to noble metals loaded on the $CuGa_3S_5$ surface, and NiS particles dispersed in the reaction solution cannot accept the electrons. It is thus believed that NiS does not function as an additional reduction cocatalyst but only interferes with light absorption by Pt- or Rh-loaded $CuGa_3S_5$.

3.4. Reaction Mechanism. On the basis of the above results, the reaction mechanism of the photocatalytic H_2 evolution from $CuGa_3S_5$ is schematically depicted in Figure 10. In H_2 evolution by $CuGa_3S_5$ loaded with noble metal cocatalysts (Figure 10A), $CuGa_3S_5$ absorbs photons with energy greater than the band gap, generating electrons and holes in the conduction and valence bands, respectively. The conduction band electrons are effectively injected into the noble metal cocatalysts deposited on the $CuGa_3S_5$ surface to reduce adsorbed H^+ into H_2, whereas holes in the valence band oxidize S^{2-} and SO_3^{2-} on the surface of $CuGa_3S_5$. Presumably, the electron-transfer process from $CuGa_3S_5$ to the loaded noble metals is too fast to allow for electron injection into the NiS particles dispersed in the reactant solution, as suggested by the results shown in Figure 9. In unloaded $CuGa_3S_5$, however, the conduction band electrons are able to migrate to the dispersed NiS particles through mechanical collisions in the stirred suspension, even though there is no physical junction between the $CuGa_3S_5$ and NiS particles (Figure 10B). Finally, water reduction occurs on the NiS particles to give H_2 molecules.

The interfacial structure between a cocatalyst and a photocatalyst is important for the prompt migration of photogenerated electrons, which results in an efficient photocatalytic reaction.[9,14,15,29,30] The results of the present study, however, demonstrate that it is possible to realize efficient photocatalysis without an intimate junction between the cocatalyst and photocatalyst. Nevertheless, the effectiveness of such a system is dependent on the particular cocatalyst and photocatalyst employed. These findings present a new opportunity for the design of the interfacial structure at which charge injection occurs.

4. Conclusions

Copper gallium sulfide ($CuGa_3S_5$), prepared by a solid-state reaction, showed photocatalytic H_2 evolution activity under visible-light irradiation ($\lambda > 420$ nm) from an aqueous solution containing S^{2-} and SO_3^{2-} as sacrificial electron donors. Irradiation of an aqueous Na_2S and Na_2SO_3 suspension containing $CuGa_3S_5$ and NiS with visible light resulted in an improved rate of H_2 evolution, 3 times that achieved in a similar reaction system using an optimized noble metal (Rh)/$CuGa_3S_5$ photocatalyst without NiS. Under irradiation by light with energy greater or equivalent to the band gap of $CuGa_3S_5$ (ca. 2.4 eV), electrons and holes are generated in the conduction and valence bands of $CuGa_3S_5$, respectively. The photogenerated electrons are able to migrate to NiS particles suspended in the reactant solution to reduce water, while the holes are scavenged by S^{2-} and SO_3^{2-} ions. The entire process, including electron migration from $CuGa_3S_5$ to NiS and subsequent H_2 evolution on NiS, is more facile than in a noble metal (e.g., Rh, Pt, and Ir)-loaded $CuGa_3S_5$, in which the process is generally believed to be efficient.

Acknowledgment. This work was supported by the Research and Development in a New Interdisciplinary Field Based on Nanotechnology and Materials Science program of the Ministry of Education, Culture, Sports, Science, and Technology (MEXT) of Japan, and The KAITEKI Institute, Inc.

References and Notes

(1) (a) Lee, J. S. *Catal. Surv. Asia* **2005**, *9*, 217. (b) Maeda, K.; Domen, K. *J. Phys. Chem. C* **2007**, *111*, 7851. (c) Osterloh, F. E. *Chem. Mater.* **2008**, *20*, 35. (d) Kudo, A.; Miseki, Y. *Chem. Soc. Rev.* **2009**, *38*, 253. (e) Youngblood, W. J.; Lee, S.-H. A.; Maeda, K.; Mallouk, T. E. *Acc. Chem. Res.* **2009**, *42*, 1966.

(2) (a) Kato, H.; Asakura, K.; Kudo, A. *J. Am. Chem. Soc.* **2003**, *125*, 3082. (b) Sakata, Y.; Matsuda, Y.; Yanagida, T.; Hirata, K.; Imamura, H.; Teramura, K. *Catal. Lett.* **2008**, *125*, 22.

(3) (a) Matsumura, M.; Saho, Y.; Tsubomura, H. *J. Phys. Chem.* **1983**, *87*, 3807. (b) Reber, J. F.; Meier, K. *J. Phys. Chem.* **1986**, *90*, 824.

(4) Kudo, A.; Sekizawa, M. *Chem. Commun.* **2000**, 1371.

(5) (a) Tsuji, I.; Kato, H.; Kobayashi, H.; Kudo, A. *J. Am. Chem. Soc.* **2004**, *126*, 13406. (b) Tsuji, I.; Kato, H.; Kobayashi, H.; Kudo, A. *J. Phys. Chem. B* **2005**, *109*, 7323.

(6) Tsuji, I.; Kato, H.; Kudo, A. *Angew. Chem., Int. Ed.* **2005**, *44*, 3565.

(7) Jang, J. S.; Choi, S. H.; Shin, N.; Yu, C.; Lee, J. S. *J. Solid State Chem.* **2007**, *180*, 1110.

(8) Bao, N. Z.; Shen, L. M.; Takata, T.; Domen, K. *Chem. Mater.* **2008**, *20*, 110.

(9) Jang, J. S.; Ham, D. J.; Lakshminarasimhan, N.; Choi, W.; Lee, J. S. *Appl. Catal., A* **2008**, *346*, 149.

(10) (a) Zong, X.; Yan, H.; Wu, G.; Ma, G.; Wen, F.; Wang, L.; Li, C. *J. Am. Chem. Soc.* **2008**, *130*, 7176. (b) Zong, X.; Wu, G.; Yan, H.; Ma, G.; Shi, J.; Wen, F.; Wang, L.; Li, C. *J. Phys. Chem. C* **2010**, *114*, 1963.

(11) Yan, H.; Yang, J.; Ma, G.; Wu, G.; Zong, X.; Lei, Z.; Shi, J.; Li, C. *J. Catal.* **2009**, *266*, 165.

(12) Wang, X.; Liu, G.; Chen, Z.-G.; Li, F.; Wang, L.; Lu, G. Q.; Cheng, H.-M. *Chem. Commun.* **2009**, 3452.

(13) (a) Maeda, K.; Teramura, K.; Lu, D.; Takata, T.; Saito, N.; Inoue, Y.; Domen, K. *Nature* **2006**, *440*, 295. (b) Maeda, K.; Teramura, K.; Saito, N.; Inoue, Y.; Domen, K. *J. Catal.* **2006**, *243*, 303. (c) Maeda, K.; Teramura, K.; Lu, D.; Saito, N.; Inoue, Y.; Domen, K. *Angew. Chem., Int. Ed.* **2006**, *45*, 7806.

(14) Maeda, K.; Saito, N.; Lu, D.; Inoue, Y.; Domen, K. *J. Phys. Chem. C* **2007**, *111*, 4749.

(15) Ogisu, K.; Ishikawa, A.; Shimodaira, Y.; Takata, T.; Kobayashi, H.; Domen, K. *J. Phys. Chem. C* **2008**, *112*, 11978.

(16) (a) Abrahams, S. C.; Bernstein, J. L. *J. Chem. Phys.* **1973**, *59*, 5415. (b) Brandt, G.; Raeuber, A.; Schneidr, J. *Solid State Commun.* **1973**, *12*, 481.

(17) (a) Ishikawa, A.; Takata, T.; Kondo, J. N.; Hara, M.; Kobayashi, H.; Domen, K. *J. Am. Chem. Soc.* **2002**, *124*, 13547. (b) Ishikawa, A.; Yamada, Y.; Takata, T.; Kondo, J. N.; Hara, M.; Kobayashi, H.; Domen, K. *Chem. Mater.* **2003**, *15*, 4442.

(18) Kakihara, M. *J. Sol−Gel Sci. Technol.* **1996**, *5*, 7.

(19) Kraeutler, B.; Bard, A. J. *J. Am. Chem. Soc.* **1978**, *100*, 4317.

(20) Dean, J. A., Ed. *Lange's Handbook of Chemistry*, 13th ed.; McGraw-Hill Book Company: New York, 1985.

(21) Miyasaka, T.; Kijitori, Y.; Murakami, N.; Kimura, M.; Uegusa, S. *Chem. Lett.* **2002**, *31*, 1250.

(22) Shannon, R. D. *Acta Crystallogr., Sect. A* **1976**, *32*, 751.

(23) (a) Zhang, S. B.; Wei, S. H.; Zunger, A. *Phys. Rev. B* **1998**, *57*, 9642. (b) Fearheiley, M. L. *Sol. Cells* **1986**, *16*, 91. (c) Bachmann, K. J.; Fearheiley, M.; Shing, Y. H.; Tan, N. *Appl. Phys. Lett.* **1984**, *44*, 407.

(24) (a) Djellal, L.; Omeiri, S.; Trari, M. *J. Alloys Compd.* **2009**, *476*, 584. (b) Neumann, B.; Bogdanoff, P.; Tributsch, H. *J. Phys. Chem. C* **2009**, *113*, 20980.

(25) (a) Vandenborre, H.; Vermeiren, P.; Leysen, R. *Electrochim. Acta* **1984**, *29*, 297. (b) Gonzalez, E. R.; Avaca, L. A.; Tremiliosi, G.; Machado, S. A. S.; Ferreira, M. *Int. J. Hydrogen Energy* **1994**, *19*, 17. (c) Assuncao, N. A.; Giz, M. J.; Tremiliosi, G.; Gonzalez, E. R. *J. Electrochem. Soc.* **1997**, *144*, 2794.

(26) Serpone, N.; Borgarello, E.; Grätzel, M. *J. Chem. Soc., Chem. Commun.* **1984**, 342.

(27) Sobczynski, A.; Bard, A. J.; Campion, A.; Fox, M. A.; Mallouk, T. E.; Webber, S. E.; White, J. M. *J. Phys. Chem.* **1987**, *91*, 3316.

(28) Yoshimura, J.; Kudo, A.; Tanaka, A.; Domen, K.; Maruya, K.; Onishi, T. *Chem. Phys. Lett.* **1988**, *147*, 401.

(29) Hara, M.; Nunoshige, J.; Takata, T.; Kondo, J. N.; Domen, K. *Chem. Commun.* **2003**, 3000.

(30) Shimodaira, Y.; Kudo, A.; Kobayashi, H. *Chem. Lett.* **2007**, *36*, 170.

JP103158F